HHS Public Access

Author manuscript

Cell Rep. Author manuscript; available in PMC 2016 March 09.

Published in final edited form as:

Cell Rep. 2016 March 8; 14(9): 2084–2091. doi:10.1016/j.celrep.2016.01.075.

Poxviruses Encode a Reticulon-Like Protein that Promotes Membrane Curvature

Karl J. Erlandson[1,4], **Himani Bisht**[1,4,!], **Andrea S. Weisberg**[1], **Seong-In Hyun**[1], **Bryan T. Hansen**[2], **Elizabeth R. Fischer**[2], **Jenny E. Hinshaw**[3], and **Bernard Moss**[1,*]

[1]Laboratory of Viral Diseases, National Institute of Allergy and Infectious Diseases, National Institutes of Health, Bethesda, MD 20892

[2]Research Technologies Branch, Rocky Mountain Laboratories, National Institute of Allergy and Infectious Diseases, National Institutes of Health, Hamilton, MT 59840

[3]Structural Cell Biology Section, National Institute of Diabetes and Digestive and Kidney Diseases, National Institutes of Health, Bethesda, MD 20892

[4]Co-first author

Abstract

Poxviruses are enveloped DNA viruses that replicate within the cytoplasm. The first viral structures are crescents and spherical particles with a lipoprotein membrane bilayer thought to be derived from the endoplasmic reticulum (ER). We determined that A17, a conserved viral transmembrane protein essential for crescent formation, forms homo-oligomers and shares topological features with cellular reticulon-like proteins, which promote membrane curvature and contribute to the tubular structure of the ER. When the purified A17 protein was incorporated into liposomes, 25 nm diameter vesicles and tubules formed at low and high A17 concentrations, respectively. In addition, intracellular expression of A17, in the absence of other viral structural proteins, transformed the ER into aggregated 3-dimensional tubular networks. We suggest that A17 is a viral reticulon-like protein that contributes to curvature during biogenesis of the poxvirus membrane.

INTRODUCTION

Enveloped viruses have curved lipoprotein membranes that are typically acquired from the host cell by budding or by wrapping of cellular cisternae. Poxviruses are exceptional in that the first distinct membrane structures appear as crescents or cupules, comprised of a single

*Correspondence: bmoss@nih.gov.

!Current Address: Center for Devices and Radiological Health, Food and Drug Administration

AUTHOR CONTRIBUTIONS

KJE, HB, ASW, SH, BTH and ERF conducted the experiments; KJE, HB, ASW, JEH and BM designed the experiments; KJE and BM wrote the paper.

membrane bilayer unconnected to cellular membranes (Dales and Mosbach, 1968). Nevertheless, the association of some viral proteins with the endoplasmic reticulum (ER) and ER-Golgi intermediate compartment (ERGIC) suggest that cellular organelles may serve as viral membrane precursors (Husain et al., 2006; Krijnse-Locker et al., 1996; Salmons et al., 1997). Studies with conditional lethal mutants of the prototype poxvirus, vaccinia virus (VACV), identified several viral proteins with direct roles in crescent membrane formation. Morphogenesis is impaired and small vesicles or tubules accumulate when the VACV major transmembrane (TM) proteins A14 or A17 are repressed (Rodriguez et al., 1997; Rodriguez et al., 1998; Traktman et al., 2000; Wolffe et al., 1996). When the genes encoding several other small viral proteins are deleted or repressed, the VACV crescent membranes remain continuous with the ER and immature virion (IV)-like structures pinch off and are trapped within the expanded ER lumen (Maruri-Avidal et al., 2013). The above genetic and microscopic data, together with biochemical studies (Husain et al., 2006), support an ER origin of the viral membrane.

Generation of local membrane curvature is often involved in remodeling and fusion of membranes. On searching for poxviral membrane proteins that could contribute to curvature, we noted that the conserved A17 protein has predicted features that strongly resemble the reticulon homology domain of cellular reticulons and DP1/Yop1p, which are involved in tubulation of the ER (Voeltz et al., 2006). The yeast and mammalian reticulons have no sequence homology to each other but form characteristic hairpin structures in the ER membrane that cause tubule formation when overexpressed. In the present study we show that liposomes reconstituted with the VACV A17 protein formed 25 nm vesicles and tubules that resembled the size and shape of viral structures formed in cells infected with VACV in the absence of the A14 membrane protein, although the latter structures contain additional viral proteins (Bisht et al., 2009; Rodriguez et al., 1997; Traktman et al., 2000). Furthermore, expression of A17 in uninfected cells or infected cells (under conditions that prevented the synthesis of A14 and other components of the virion membrane) promoted the formation of aggregated 3-dimensional tubular ER networks. Similar networks containing A17 and ER marker proteins were detected in some cells when formation of virions was perturbed during infection with certain mutant viruses. We propose that the poxvirus-encoded reticulon-like protein contributes to curvature during an early stage of viral membrane biogenesis.

RESULTS

A17 Has Conserved Features of Reticulons

The reticulons and DP1/Yop1p have no significant amino acid sequence identity but share a conserved domain of 200 amino acid residues comprised of hydrophobic segments that insert into one side of the membrane forming a wedge and inducing curvature as depicted in Figure 1C (Shibata et al., 2009). To identify VACV proteins that could similarly contribute to membrane curvature, the Tied Mixture Hidden Markov Model (TMHMM) program (Krogh et al., 2001), which predicts likely TM sequences, was used to screen the VACV proteome. Yop1p served as a template to search for proteins with at least 30 consecutive amino acids predicted to be within the membrane. The only expressed VACV-encoded

protein that met this standard was A17, which is highly conserved in chordopoxviruses and is required for viral membrane formation. A17, like Yop1p and reticulons, has four hydrophobic domains (Fig. 1A) of which the first two comprising residues 62-103 were predicted by TMHMM and Octopus (Viklund and Elofsson, 2008) programs to be one long TM segment. The predicted membrane profile of A17 was strikingly similar to the reticulons and DP1/Yop1p (Fig. 1B).

Evidence for the topology of reticulons was obtained upon substituting cysteines for other amino acids in the hydrophilic segment between the two hairpins and demonstrating their accessibility to membrane impermeable maleimide-polyethylene glycol in the presence of low concentrations of digitonin by altered electrophoretic mobility (Voeltz et al., 2006). Using a similar strategy, we found partial mobility shifts of A17 with cysteine substitutions of amino acids 38, 108 and 109 suggesting that they face the cytoplasm (Fig. S1). The hairpin model is also consistent with previous findings that the N- and C- termini of A17 face the cytoplasm (Betakova and Moss, 2000; Betakova et al., 1999; Krijnse-Locker et al., 1996) and that cysteines 101 and 121 can form an intramolecular disulfide bond within adjacent helices in the membrane, although previously interpreted differently (Betakova and Moss, 2000). However, we cannot rule out the possibility that a few amino acids are luminal at the apex of each hairpin.

Expression and Purification of the A17 Protein

The apparently similar topologies of A17 and Yop1p encouraged us to purify and further characterize the viral protein. For expression of A17 in *Escherichia coli*, we considered it prudent to remove the three cysteines (asterisks in Figure 1A), which were previously found to be unnecessary for VACV infectivity (Betakova and Moss, 2000), to prevent the possibility of spurious disulfide bond formation. In addition, as we planned to append histidine residues to A17 to facilitate purification, we investigated the effect of this addition on biological activity. Synthesis of A17 and the N- and C-terminal histidine modified forms was demonstrated by transfecting expression plasmids into cells infected with a conditionally lethal inducible A17 virus (Wolffe et al., 1996) in the absence of inducer and probing Western blots with antibody to A17 (Fig. 1D). Proteolytic processing of the N- and C-termini of A17 occurs during morphogenesis resulting in incompletely resolved products that usually appear as two bands. There was less processing of A17 expressed by transfection, particularly in the N-terminal His-A17, than in the control in which the inducer IPTG was added (Fig. 1D). Nevertheless, both the unmodified and histidine-modified A17 proteins increased infectivity of the inducible mutant above that of the input virus in the mock-transfection control (Fig. 1E). Therefore, we proceeded to produce N- and C-terminally His-tagged codon-optimized A17 proteins in *E. coli* (Fig. S2). The yield of the full-length protein solubilized in the detergent Fos-choline 12 was higher with the N-terminal tagged version, the purity of which is shown in Figure 1F.

Homo-oligomerization is another important characteristic of reticulons and DPI/Yop1p that contributes to their ability to promote tubule formation. Following the procedure of Shibata et al. (Shibata et al., 2008), we incubated purified A17 in liposomes with the cross-linker ethylene glycol bis(succinimidyl succinate (EGS). The formation of A17 multimers with

increasing concentrations of EGS was shown by electrophoresis and Western blotting (Fig. 1G). Oligomers were also demonstrated in cellular membranes. Cells were infected with a recombinant VACV that expresses T7 RNA polymerase and transfected with a plasmid encoding A17 regulated by a T7 promoter in the presence of a DNA replication inhibitor to prevent synthesis of other viral structural proteins. The membrane fraction was treated with EGS and analyzed as above to show A17 multimers (Fig. 1H).

A17 Promotes Tubule Formation *In Vitro*

To determine the interaction between A17 and membranes *in vitro*, we closely followed the procedures used for demonstrating tubule formation by reticulons (Hu et al., 2008). Purified A17 was mixed with detergent-solubilized *E. coli* polar lipids and the detergent slowly removed by dialysis. In the absence of A17, the vesicles produced were of various sizes with no distinct morphology (Figure 2A). When A17 was added, there was an enrichment of vesicles and tubules with diameters of 25 nanometers (Figure 2B, S3A). Raising the concentration of A17 relative to lipids enhanced the formation of tubules (Figure 2C, 2D), which increased in length as the ratio of A17:lipid reached 1:1 (w/w) (Figure S3B). These data indicated that the curvature can be extended along the length of the tubule, likely due to homo-oligomerization of A17, similar to that proposed for the reticulons (Shibata et al., 2009). The localization of A17 along the tubules was demonstrated by immune-EM using antibody to A17 followed by protein A conjugated to gold spheres (Figure 2E). Tubule formation was also demonstrated when the His-tag was removed (Figure 2F) and when ER lipids were used instead of *E. coli* lipids (Figure 2G). As a negative control, we also expressed and purified the His-tagged form of A14, another major VACV transmembrane protein that does not resemble reticulons. In contrast to A17, neither specific size vesicles nor tubules formed with A14 (data not shown).

Expression of the A17 Protein Promotes Formation of ER Networks

During a productive infection, VACV usurps the translational apparatus of the cell and synthesizes structural proteins at high levels within specialized cytoplasmic factories. The A17 protein is expressed late in infection and is one of the five most abundant proteins associated with virions (Resch et al., 2007). A scheme was devised to analyze the effect of high levels of A17 on the structure of the ER in the absence of the other abundant viral membrane proteins. In this way we could prevent further steps in viral membrane formation. A plasmid encoding the A17 ORF regulated by a bacteriophage T7 promoter was transfected into cells that had been infected with a recombinant VACV that expresses bacteriophage T7 RNA polymerase (Fuerst et al., 1986). The infections were carried out in the presence of cytosine arabinoside (AraC) to prevent viral DNA replication and subsequent expression of A14 and other viral membrane proteins. When A17 was expressed, the ER was modified to form complex networks (Figure 3, panels 1, 4) which were not observed when the empty vector plasmid was transfected (Figure 3, panel 2). Furthermore, VACV infection was not required since similar networks formed when A17 was overexpressed by transfecting the plasmid into a cell line that constitutively expressed T7 RNA polymerase (Figure 3, panel 3). Evidence that the A17-induced networks contained A17 (Fig. 3, panel 5) and the ER intraluminal protein disulfide isomerase (Fig. 3, panel 6) was obtained by immune-electron microscopy.

The A17-ER networks were not discerned in cells infected with wild-type VACV, in which viral particles are actively being formed. However, we considered that these structures might form and persist under conditions in which development of normal viral membranes from the ER is impaired. Therefore, we examined images from cells infected with a variety of conditional lethal VACV mutants. Although not reported in the original publications (Resch et al., 2005; Satheshkumar et al., 2009) because of their infrequent occurrence, we did find examples of A17-ER networks when synthesis of A11 (Figure 3, panel 7) or H7 (not shown) was repressed. The identity of the structures that formed when A11 was repressed was confirmed by labeling with antibodies to A17 (Figure 3, panel 8) and to the ER marker protein disulfide isomerase (Fig. 3, panel 9). Aberrant viral membrane structures are also formed from the ER under these conditions probably accounting for the absence of large A17-ER networks in most of the cells infected with the mutants.

Visualization of A17-ER Networks by Tomography

Tomography was employed to visualize the altered ER in three dimensions. The ER networks, formed in infected cells after transfection of a plasmid expressing A17, appeared as tangles of branching, twisting, sheets and tubules that were continuous with the rest of the ER in the cytoplasm (Figure 4, Rows 1, 2; Movies S1, S2) and with the nuclear envelope (Figure 4, Row 3; Movie S3). Tubules were apparent in cross-sections (Movie S3).

DISCUSSION

Recent studies indicate that the VACV membrane forms from the ER by a poorly understood mechanism that involves multiple viral proteins, the functions of which remain to be fully elucidated (Moss, 2015). Here, we focused on the A17 protein, which is highly conserved in chordopoxviruses and is essential for viral membrane formation. The starting point for the present study was our observation that A17 has features that resemble the reticulons and DP1/Yop1p. Although there is no significant amino acid sequence identity between the reticulons and DP1/Yop1p, they share the following characteristics: (1) ability to cause membrane tubulation in vitro, (2) association with tubular ER in cells, (3) topology – insertion of two hairpins in the membrane with no or minimal luminal exposure and (4) homo-oligomerization (Shibata et al., 2009). The insertion of hairpins is thought to displace more lipid head groups on one side of the membrane, inducing curvature as diagrammed in Figure 1C. This wedge effect plus oligomerization promotes tubule formation. A17, the reticulons and DPI/Yop1p all share two relatively long, 30- to 40-amino acids, stretches of hydrophobic residues in a 200 amino acid domain. Both bioinformatics and topological studies suggested that the transmembrane segments of A17 also form hairpins in the membrane. In addition, homo-oligomerization of A17 was demonstrated by cross-linking purified A17 in liposomes and A17 expressed in cells and associated with membranes.

In the first part of this study, we incorporated purified A17 protein into liposomes following the procedures used for Yop1p (Hu et al., 2008). Spheres and tubules formed at similar protein/lipid molar ratios of A17 and Yop1p with diameters of 25 nm and 15 to 17 nm, respectively. The lengths of the tubules increased with protein concentration, reaching lengths of several hundred nanometers at comparable protein/lipid ratios for both A17 and

Yop1p. Interestingly, the A17 vesicles and tubules were similar in size to structures containing A17 that are found during VACV infection when the other major transmembrane protein, A14, is repressed and viral membrane formation is prevented (Rodriguez et al., 1998; Traktman et al., 2000; Unger et al., 2013). We propose that a scaffold of A17 molecules is formed at high concentrations, extending the curvature along the length of the tubule, similar to the mechanism proposed for reticulons. It has previously been shown that only 10% of the tubule surface would need to be occupied by reticulon-like protein to extend and stabilize tubules (Hu et al., 2011).

The major structural proteins of VACV, including A17, are normally expressed at high levels in specialized viral factories following genome replication. In addition to viral genomes and proteins, these factories contain ER, mitochondria and other cellular organelles. During a productive virus infection, A17 can be mainly detected in association with nascent viral membranes as well as immature and mature virions (Rodriguez et al., 1997; Wolffe et al., 1996). We considered that modification of cellular membranes by A17 might be discerned by expressing the protein early in infection and preventing genome replication and the consequent synthesis of other structural proteins, which would lead to viral envelope formation. This plan was accomplished by infecting cells with a VACV recombinant virus that expresses T7 RNA polymerase in the presence of a DNA replication inhibitor and transfecting a plasmid encoding A17 regulated by the bacteriophage T7 promoter. Under these conditions, there was a remarkable change in appearance of the ER, which formed a network resembling a ball of yarn. The presence in these structures of both A17 and an ER luminal protein was confirmed by immune-electron microscopy. By tomography, the network appeared as branched, highly curved sheets and tubules having continuity with the rest of the cytoplasmic ER and nuclear envelope. Similar A17-ER networks formed when the plasmid was transfected into uninfected cells stably expressing T7 RNA polymerase, confirming that no other viral proteins were needed. We also found these networks in occasional cells infected with certain virus mutants that have defects in synthesis of other proteins involved in envelope formation. In the latter situation, A17 was expressed from the viral genome under its natural promoter. Thus, A17 has an intrinsic ability to associate with the ER and dramatically alter its structure, which was revealed by perturbing later steps in viral envelope formation. Presumably, A17-modified ER is recruited to form viral envelopes before large networks can form during a natural infection.

EXPERIMENTAL PROCEDURES

Liposome Reconstitution Assay

Purified A17 was reconstituted with *E. coli* polar lipids or a mixture of lipids mimicking the ER Detergent was removed by dialysis and droplets were stained with uranyl acetate on carbon-coated Rh Flashed Copper mesh grids. For immunogold labeling, grids were blocked with bovine serum albumin and incubated with primary antibody followed by protein A-10 nm gold.

Electron Microscopy of Infected and Transfected cells

RK-13 or BS-C-1 cells were infected with vTF7-3 (Fuerst et al., 1986) and after 1 h were transfected with a plasmid encoding the A17 ORF regulated by a T7 promoter. After 16 h the cells were fixed and prepared for transmission electron microscopy. Alternatively, a BHK-21 cell clone (BSR-T7/5) that expresses T7 RNA polymerase (Habjan et al., 2008) was transfected with the plasmid pVOTE1-A17L, which was derived from pVOTE1 (Ward et al., 1995) and expresses the A17 ORF regulated by the T7 promoter. For tomography, tilt images of 200-nm-thick sections were collected using a Tecnai BioTwin Spirit TEM (FEI) operated at 120 kV. Additional experimental details are provided in the Supplemental Material.

Cross-linking

Methods were modified from Shibata and coworkers (Shibata et al., 2008). For both cell- and in vitro-derived membranes, samples were treated with 0 to 2 mM EGS at room temperature for 30 min. and analyzed by electrophoresis on a 4 to 12% Bis-Tris NuPAGE gel (Invitrogen). The A17 protein was visualized with anti-A17N antibody and donkey anti-rabbit IRDye800CW (Li-Cor)

Supplementary Material

Refer to Web version on PubMed Central for supplementary material.

ACKNOWLEDGEMENTS

Support was from the Division of Intramural Research, NIAID. KJE received support from a NIGMS PRAT fellowship.

REFERENCES

Betakova T, Moss B. Disulfide bonds and membrane topology of the vaccinia virus A17L envelope protein. J Virol. 2000; 74:2438–2442. [PubMed: 10666276]

Betakova T, Wolffe EJ, Moss B. Membrane topology of the vaccinia virus A17L envelope protein. Virology. 1999; 261:347–356. [PubMed: 10497120]

Bisht H, Weisberg AS, Szajner P, Moss B. Assembly and disassembly of the capsid-like external scaffold of immature virions during vaccinia virus morphogenesis. J Virol. 2009; 83:9140–9150. [PubMed: 19570860]

Dales S, Mosbach EH. Vaccinia as a model for membrane biogenesis. Virology. 1968; 35:564–583. [PubMed: 5677800]

Fuerst TR, Niles EG, Studier FW, Moss B. Eukaryotic transient-expression system based on recombinant vaccinia virus that synthesizes bacteriophage T7 RNA polymerase. Proc Natl Acad Sci USA. 1986; 83:8122–8126. [PubMed: 3095828]

Habjan M, Penski N, Spiegel M, Weber F. T7 RNA polymerase-dependent and - independent systems for cDNA-based rescue of Rift Valley fever virus. J Gen Virol. 2008; 89:2157–2166. [PubMed: 18753225]

Hu J, Prinz WA, Rapoport TA. Weaving the web of ER tubules. Cell. 2011; 147:1226–1231. [PubMed: 22153070]

Hu J, Shibata Y, Voss C, Shemesh T, Li Z, Coughlin M, Kozlov MM, Rapoport TA, Prinz WA. Membrane proteins of the endoplasmic reticulum induce high-curvature tubules. Science. 2008; 319:1247–1250. [PubMed: 18309084]

Husain M, Weisberg AS, Moss B. Existence of an operative pathway from the endoplasmic reticulum to the immature poxvirus membrane. Proc Natl Acad Sci USA. 2006; 103:19506–19511. [PubMed: 17146047]

Krijnse-Locker J, Schleich S, Rodriguez D, Goud B, Snijder EJ, Griffiths G. The role of a 21-kDa viral membrane protein in the assembly of vaccinia virus from the intermediate compartment. J Biol Chem. 1996; 271:14950–14958. [PubMed: 8662995]

Krogh A, Larsson B, von Heijne G, Sonnhammer EL. Predicting transmembrane protein topology with a hidden Markov model: application to complete genomes. J Mol Biol. 2001; 305:567–580. [PubMed: 11152613]

Maruri-Avidal L, Weisberg AS, Moss B. Direct formation of vaccinia viral membranes from the endoplasmic reticulum in the absence of the newly characterized L2-interacting A30.5 protein. J Virol. 2013; 87:12313–12326. [PubMed: 24027302]

Moss B. Poxvirus membrane biogenesis. Virology. 2015; 479-480:619–626. [PubMed: 25728299]

Resch W, Hixson KK, Moore RJ, Lipton MS, Moss B. Protein composition of the vaccinia virus mature virion. Virology. 2007; 358:233–247. [PubMed: 17005230]

Resch W, Weisberg AS, Moss B. Vaccinia virus nonstructural protein encoded by the A11R gene is required for formation of the virion membrane. J Virol. 2005; 79:6598–6609. [PubMed: 15890898]

Rodriguez JR, Risco C, Carrascosa JL, Esteban M, Rodriguez D. Characterization of early stages in vaccinia virus membrane biogenesis: implications of the 21-kilodalton protein and a newly identified 15-kilodalton envelope protein. J Virol. 1997; 71:1821–1833. [PubMed: 9032312]

Rodriguez JR, Risco C, Carrascosa JL, Esteban M, Rodriguez D. Vaccinia virus 15-kilodalton (A14L) protein is essential for assembly and attachment of viral crescents to virosomes. J Virol. 1998; 72:1287–1296. [PubMed: 9445029]

Salmons T, Kuhn A, Wylie F, Schleich S, Rodriguez JR, Rodriguez D, Estban M, Griffiths G, Locker JK. Vaccinia virus membrane proteins p8 and p16 are cotranslationally inserted into the rough endoplasmic reticulum and retained in the intermediate compartment. J Virol. 1997; 71:7404–7420. [PubMed: 9311819]

Satheshkumar PS, Weisberg A, Moss B. Vaccinia virus H7 protein contributes to the formation of crescent membrane precursors of immature virions. J Virol. 2009; 83:8439–8450. [PubMed: 19553304]

Shibata Y, Hu J, Kozlov MM, Rapoport TA. Mechanisms shaping the membranes of cellular organelles. Annu Rev Cell Dev Biol. 2009; 25:329–354. [PubMed: 19575675]

Shibata Y, Voss C, Rist JM, Hu J, Rapoport TA, Prinz WA, Voeltz GK. The reticulon and DP1/Yop1p proteins form immobile oligomers in the tubular endoplasmic reticulum. J Biol Chem. 2008; 283:18892–18904. [PubMed: 18442980]

Traktman P, Liu K, DeMasi J, Rollins R, Jesty S, Unger B. Elucidating the essential role of the A14 phosphoprotein in vaccinia virus morphogenesis: Construction and characterization of a tetracycline-inducible recombinant. J Virol. 2000; 74:3682–3695. [PubMed: 10729144]

Unger B, Mercer J, Boyle KA, Traktman P. Biogenesis of the vaccinia virus membrane: genetic and ultrastructural analysis of the contributions of the A14 and A17 proteins. J Virol. 2013; 87:1083–1097. [PubMed: 23135725]

Viklund H, Elofsson A. OCTOPUS: improving topology prediction by two-track ANN-based preference scores and an extended topological grammar. Bioinformatics. 2008; 24:1662–1668. [PubMed: 18474507]

Voeltz GK, Prinz WA, Shibata Y, Rist JM, Rapoport TA. A class of membrane proteins shaping the tubular endoplasmic reticulum. Cell. 2006; 124:573–586. [PubMed: 16469703]

Ward GA, Stover CK, Moss B, Fuerst TR. Stringent chemical and thermal regulation of recombinant gene expression by vaccinia virus vectors in mammalian cells. Proc Natl Acad Sci USA. 1995; 92:6773–6777. [PubMed: 7624318]

Wolffe EJ, Moore DM, Peters PJ, Moss B. Vaccinia virus A17L open reading frame encodes an essential component of nascent viral membranes that is required to initiate morphogenesis. J Virol. 1996; 70:2797–2808. [PubMed: 8627754]

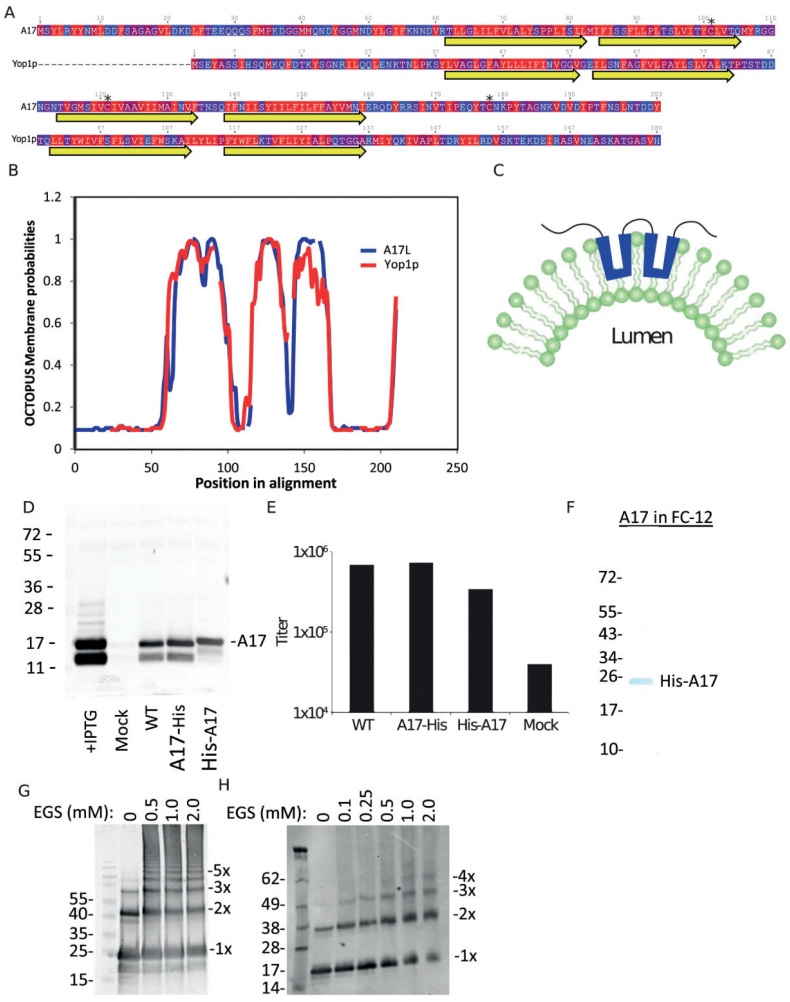

Figure 1. A17 Resembles the ER Tubule-Forming Yop1p

(A) Comparison of Yop1p and the VACV A17 amino acid sequences with potential TM domains indicated by yellow arrows. Polar and non-polar amino acids are blue and red, respectively. Cys residues in A17 are marked by asterisks. (B) Octopus membrane probabilities of A17 and Yop1p. (C) Predicted topology of A17 modeled after Yop1p. The hydrophobic sequences enter and exit the membrane on the same side rather than crossing completely through resulting in greater displacement of the lipid head groups on one side of the membrane and induction of membrane curvature. (D) Western blot of A17 from BS-C-1 cells that were mock infected or infected with a recombinant VACV (vIndA17) expressing A17 in the presence of the inducer IPTG or transfected with plasmids encoding wild-type (WT) A17 or A17 with six histidines appended to the C-terminus (A17-His) or to the N-terminus (His-A17) in the absence of IPTG. After 24 h, the cells were lysed and the proteins were solubilized with SDS and resolved by gel electrophoresis. After transfer to a membrane, the blot was probed with antibody to A17 and visualized by infrared fluorescence. The upper and lower bands represent unprocessed and processed A17, respectively. Marker proteins in kDa are indicated on the left. (E) Virus titers from BS-C-1 cells that were infected with vIndA17 in the absence of IPTG and transfected with plasmids as in panel D or mock transfected. The titer from the mock-transfected cells represents

residual input virus. (F) Codon-optimized A17 with a 6xHis affinity tag on N-terminus and all cysteines mutated to alanines was expressed in *E. coli* and membrane fractions solubilized in fos-choline size 12 (FC-12) before applying to a nickel-affinity and size exclusion columns. Purified His-A17 monomer is shown in a Simply-Blue Coomassie-stained gel. Marker proteins with masses indicated in kDa are shown on the left. (G) A17 homo-oligomers in liposomes. Purified A17 reconstituted into *E. coli* polar lipids was subjected to increasing amounts of EGS crosslinker and resolved by SDS gel electrophoresis. After membrane transfer, the blot was probed with antibody to A17 and visualized by infrared fluorescence. The lower bands represent monomeric A17 and higher bands represent crosslink-stabilized oligomers of A17 ranging from dimer to higher order oligomers. The positions of marker proteins in kDa are shown on left. (H) A17 homo-oligomers in cellular membranes. Same as in G except VACV-infected cells were transfected with plasmid encoding A17. At 21 h after infection, the cells were washed, lysed in hypotonic buffer and cleared by low speed centrifugation before pelleting the membranes and resuspending them prior to crosslinking with EGS.

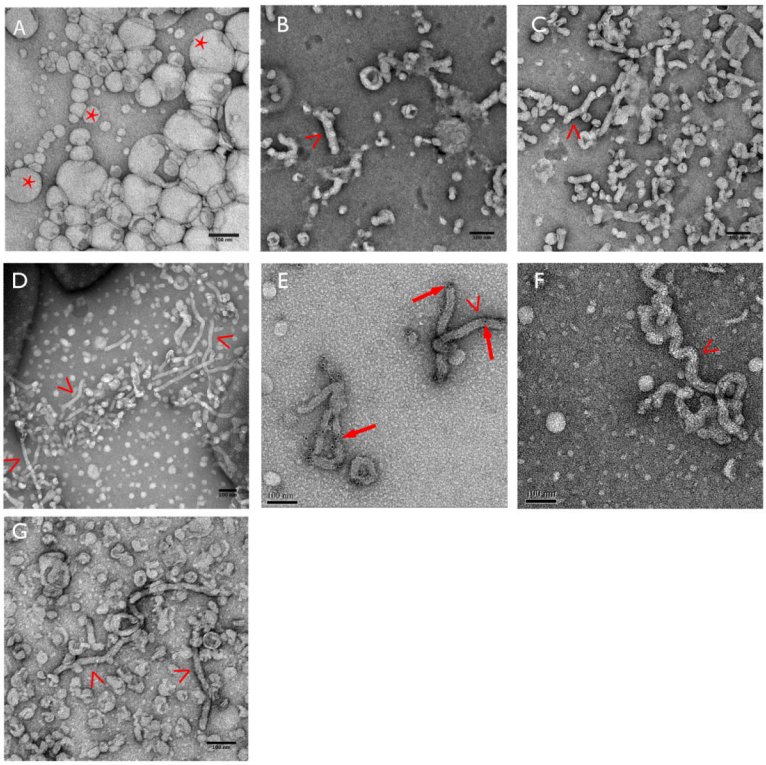

Figure 2. Constitution of Vesicles and Tubules with A17 and *E. coli* Polar Lipids

E. coli polar lipids (1 mg/ml) in the presence of FC-12 alone or 0.25 to 1.0 mg FC-12-solubilized His-A17 protein were dialyzed to remove detergent. The dialyzed materials were deposited on grids and examined by electron microscopy (A-D). Vesicles of varying sizes and morphology in the absence of A17 (A), presence of 0.25 mg/ml His-A17 (B), 0.5 mg/ml His-A17 (C) or 1.0 mg/ml of His-A17 (D). Tubules formed with *E. coli* polar lipids and His-A17 (E) or A17 with His tag removed by thrombin proteolysis (F) and then stained with antibody to A17 followed by secondary antibody conjugated to 10 nm gold. (G) Same as panel D except proteoliposomes constituted with 1 mg/ml of ER lipid mixture instead of E. coli polar lipids. Asterisks and carats point to vesicles and tubules, respectively. Arrows point to gold grains. Scale bars, 100 nm.

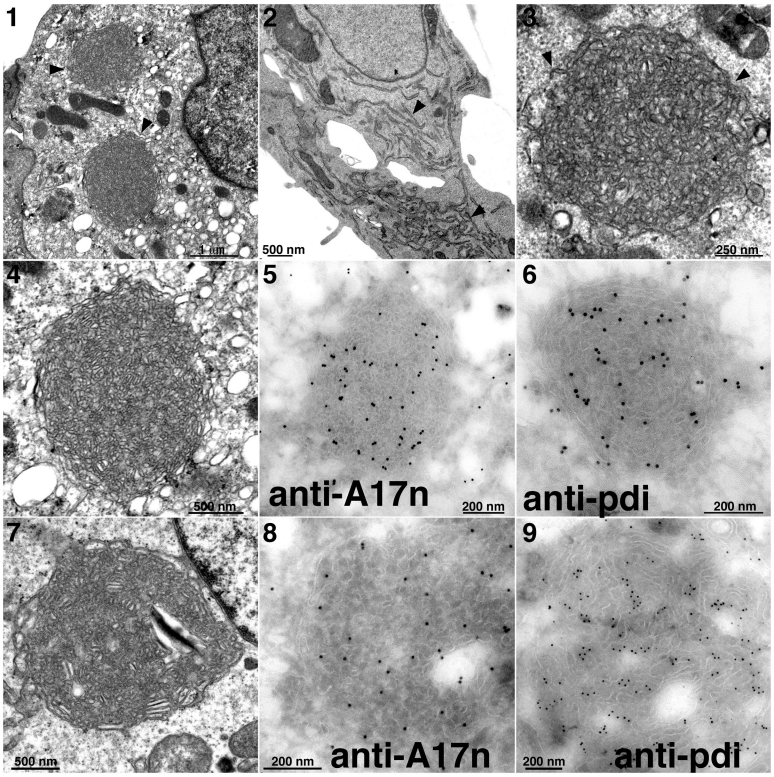

Figure 3. Overexpression of A17 Induces ER Curvature

Thin cell sections embedded in plastic were analyzed by transmission electron microscopy (panels 1-4, 7) or frozen sections were immunostained (panels 5,6, 8, 9). Arrowheads point to ER networks in panels 1 and 3 or unmodified ER in panel 2. (1) BS-C-1 cells were infected with a recombinant VACV expressing bacteriophage T7 RNA polymerase in the presence of AraC and transfected with a plasmid in which a T7 promoter regulated the A17 ORF. (2) Similar to panel 1 except that an empty vector plasmid was transfected. (3) Uninfected BHK-21 cells that stably express bacteriophage T7 RNA polymerase were transfected with a plasmid containing the A17 ORF regulated by a T7 promoter. (4) Same as panel 1 except higher magnification. (5) Immunogold labeling of networks in BS-C-1 cells infected as in panel 1 and stained with anti-A17 antibody followed by protein A conjugated to 10 nm gold. (6) RK-13 cells infected, transfected and treated as in panel 5 except that antibody was to protein disulfide isomerase. (7) BS-C-1 cells infected with a recombinant VACV with inducible A11 ORF in absence of inducer. (8) Infected as in panel 7 and stained with antibody to A17 followed by protein A conjugated to 10 nm gold. (9) Same as panel 8 except antibody was to PDI. Scale bars are shown near bottom of each panel.

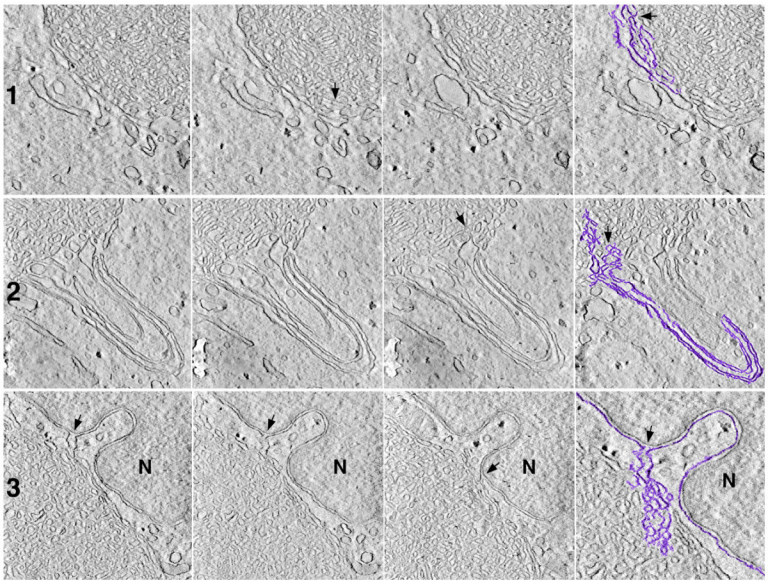

Figure 4. Visualization of ER Networks by Tomography

BS-C-1 cells were infected with a recombinant VACV expressing bacteriophage T7 RNA polymerase in the presence of AraC and transfected with a plasmid in which a T7 promoter regulated the A17 ORF as in Figure 3. Rows 1, 2 and 3 contain individual slices from tomographic data sets shown as Movies S1, S2 and S3, respectively. The arrows and colorization in the last panels of rows 1 and 2 were chosen to show the connections between uncurved and highly curved ER networks in the cytoplasm. The arrow and colorization in the last panel of row 3 shows the connection between the nuclear envelope and the highly curved network.